

## ACKNOWLEDGMENT

Financial support from a Hong Kong Polytechnic University internal grant is acknowledged.

## REFERENCES

- PILE DYNAMIC, INC. (1984, 1993). *CAPWAP Manual*. Cleveland, Ohio: Pile Dynamic, Inc.
- GEO. (1996). *Pile Design and Construction*. GEO Publication No.1/96
- GOBLE, G.G. and RAUSCHE, F. (1976). Wave Equation Analysis of Pile Driving, WEAP Program. The Case Western Reserve University, USA.
- KOLSKY, H. (1953). *Stress Waves in Solids*. S.n.: Oxford Press.
- LAW, T.S. (1996). Design and testing of the bearing capacity of driven pile in Hong Kong. M.Sc. Thesis, The Hong Kong Polytechnic University.
- LIU, M.G.; WANG, P.; PAN, Y.M.; and LIU, H. (1993). The development and application of RSM-PileStar. *Testing Technology of Pile Foundation Engineering*. S.n.: China Construction Publishing House. pp.108-118.
- LIU, M.G. (1995). Principle and design of transient, binary and floating data acquisition system. *Techniques for Measurement of Pile and Construction Site*. Hubei: Hubei Science and Technology Publishing House.
- PAQUET, J. (1992). Pile integrity testing - the CEBITP reflectogram. *Proceedings of the Conference on Piling*: London: European Practice and Worldwide Trends. pp.100-110.
- PILE DYNAMIC, INC. (1993). *PDA Manual*. Cleveland, Ohio: Pile Dynamic, Inc.
- RAUSCHE, F.; GOBLE, G.G.; and LIKINIS, G.E. Jr. (1985). Dynamic determination of pile capacity. *Journal of Geotechnical Engineering*, Vol. 111, No. 3, pp. 367-383.
- RAUSCHE, F.; MOSES, F.; and GOBLE, G.G. (1972). Soil resistance predications from pile dynamics. *Journal of Soil Mechanics and Foundation Engineering Division*, ASCE, Vol. 98.
- SMITH, E.A.L. (1955). Impact and longitudinal wave transmission. *Transaction of ASME*, pp. 963-973.
- SMITH, E.A.L. (1960). Pile driving analysis by the wave equation. *Journal of Soil Mechanics and Foundation Engineering Division*, ASCE, Vol. 86, No. SM4, pp. 35-61.
- YUAN, J.X. (1988a). On the problems of dynamic pile testing. *Journal of Rock and Soil Mechanics* Vol. 1, No. 2, pp. 2-18.
- YUAN, J.X. (1988b). Non-destructive testing methods for piles. *Journal of Rock and Soil Mechanics* Vol. 1, No. 1, pp. 83-94.

## ANALYSIS OF PILE SUBJECTED TO CYCLIC LATERAL LOADING

V. A. Sawant<sup>1</sup> and D.M. Dewaikar<sup>2</sup>

## ABSTRACT

An analysis is proposed for studying the response of a pile embedded in homogeneous clay, subjected to cyclic lateral loading, using semi-analytical finite element approach. The pile and soil media are discretized into eight nodes of isoparametric continuum elements, while interface between soil and pile is modelled using six nodes of curved interface element. Both soil and interface were modelled using bilinear stress-strain relationships. This analysis is an extension of nonlinear static pile response, and allows for reduction of soil modulus and yield pressure with number of cycles. An iterative procedure is employed, in which a constant stiffness based on initial tangent modulus of bilinear stress-strain relationship is used in all the iterations. Effect of one-way and two-way cyclic loading on moments and deflections is studied.

## INTRODUCTION

The design of offshore pile requires consideration of the effects of cyclic loading on the lateral load capacity and permanent deformation of pile head. Available methods of analysing the lateral response of piles can be broadly divided into three categories :

1. Subgrade reaction ( $p$ - $y$ ) analysis, modified for the effect of cyclic degradation by Georgiadis, et al. (1992) and Long and Venneste (1994);
2. Elastic continuum analysis modified for the effect of cyclic degradation by Poulos (1982); and
3. Finite element method by Kuhlemeyer (1979) and Randolph (1981).

Of the above approaches, the finite element method achieves a more rigorous solution than the other two methods, since the pile is modelled more accurately. Also, heterogeneous soil conditions are readily, and correctly, modelled.

The limited information available on the effects of cyclic loading on piles indicates that remarkable reduction in load capacity and pile-soil system stiffness can occur. In some of these cases, failure is characterized by a continued accumulation of permanent displacements resulting in movements of pile of the order of one pile diameter after several cycles of load application.

It appears that at least two mechanisms may contribute to the failure of piles under cyclic loading:

1. Cyclic degradation of soil modulus and yield stress; this may be expected to dominate under essentially two-way cyclic loading; and
2. Accumulation of permanent displacement with increasing load cycles; this may be expected to dominate under essentially one-way cyclic loading.

In this paper, an efficient iterative analysis based on semi-analytical finite element approach for the analysis of a laterally loaded pile embedded in clay subjected to cyclic loading, involving nonlinearity of soil and interface behavior is proposed. This analysis was an extension of the non-linear finite element analysis for static pile response, and allows for the reduction in soil modulus and yield pressure with increasing cyclic strain. For simplicity, the non-linear behavior of the soil was modelled using a bilinear stress-strain relationship. The nonlinearity of interface

<sup>1</sup> Research Scholar, Indian Institute of Technology, Bombay, Powai, Mumbai-400 076, India.

<sup>2</sup> Professor of Civil Engineering, Indian Institute of Technology, Bombay, Powai, Mumbai-400 076, India.

Note: Discussion is open until 1 July 1999. This paper is part of the *Geotechnical Engineering Journal*, Vol. 30, No. 1, April 1999. Published by the Southeast Asian Geotechnical Society, ISSN 0046-5828.

behavior was also modeled using a bilinear relationship between interface shear stress and relative shear displacement. The development of procedure was based on the evaluation of stresses and strains pertaining to constant stiffness, for various iterative steps at every cycle, involving no change in material properties in circumferential direction. The difference between the computed stress and the stress that is consistent with the computed strain in circumferential direction, was expanded in the form of a full range finite harmonic series. The expanded form of stress difference was used to compute the load vector for further iteration. Because constant modulus was employed in all the iterations, this procedure offers a unique advantage for analysing nonlinear problem through the semi-analytical approach.

### FINITE ELEMENT FORMULATION

The pile and soil media were discretized into a number of eight-node continuum elements. The interface between pile and soil was modelled using six-node interface elements developed by Buragohain and Shah (1977). Displacements  $u$ ,  $v$  and  $w$  in  $r$ ,  $\theta$  and  $z$  directions are expressed as:

$$u = \sum_{n=0}^L \bar{u}_n \cos n\theta + \sum_{n=1}^L \bar{u}_n \sin n\theta \quad (1)$$

$$v = \sum_{n=1}^L \bar{v}_n \sin n\theta + \sum_{n=0}^L \bar{v}_n \cos n\theta \quad (2)$$

$$w = \sum_{n=0}^L \bar{w}_n \cos n\theta + \sum_{n=1}^L \bar{w}_n \sin n\theta \quad (3)$$

where,  $(\bar{u}_n, \bar{v}_n, \bar{w}_n)$  and  $(\bar{u}_n, \bar{v}_n, \bar{w}_n)$  represent displacements in the  $n$ th harmonic for symmetric and antisymmetric modes respectively, and  $L$  is the total number of harmonics considered in the series. The displacements in the plane forming solid of revolution were expressed using shape functions, as employed in two-dimensional finite element formulation. Components of surface traction,  $f_u, f_v$  and  $f_w$ , in  $r, \theta$  and  $z$  directions are given as:

$$f_u = \sum_{n=0}^L \bar{f}_{un} \cos n\theta + \sum_{n=1}^L \bar{f}_{un} \sin n\theta \quad (4)$$

$$f_v = \sum_{n=1}^L \bar{f}_{vn} \sin n\theta + \sum_{n=0}^L \bar{f}_{vn} \cos n\theta \quad (5)$$

$$f_w = \sum_{n=0}^L \bar{f}_{wn} \cos n\theta + \sum_{n=1}^L \bar{f}_{wn} \sin n\theta \quad (6)$$

where  $\bar{f}_{un}, \bar{f}_{vn}$  and  $\bar{f}_{wn}$  are the amplitudes of the surface traction for  $n$ th harmonic in symmetric mode and  $\bar{f}_{un}, \bar{f}_{vn}$  and  $\bar{f}_{wn}$  are the amplitudes of the surface traction in antisymmetric mode for  $n$ th harmonic.

### Continuum Element

Relation between strains and nodal displacements is expressed as:

$$\{\epsilon\}_e = [B]\{\delta\}_e \quad (7)$$

where,  $\{\epsilon\}_e$  is the strain vector,  $\{\delta\}_e$  is a vector consisting of nodal displacements, and  $[B]$  represents the strain-displacement transformation matrix.

The stress-strain relation is given by,

$$\{\sigma\}_e = [D]\{\epsilon\}_e \quad (8)$$

where,  $\{\sigma\}_e$  is the stress vector, and  $[D]$  is the constitutive relation matrix.

The stiffness matrix,  $[k]_e$ , of an element is given as:

$$[k]_e = \int_v [B]^T [D] [B] dv \quad (9)$$

### Interface Element

The relative displacements (strains) between the surfaces of soil and structure induce stresses in the interface element. These relative displacements are given as:

$$\{\epsilon\}_e = [B]_f \{\delta\}_e \quad (10)$$

where,  $[B]_f$  represents the strain-displacement transformation matrix.

The element stiffness is obtained by the usual expression,

$$[k]_e = \int [B]_f^T [D] [B]_f ds \quad (11)$$

where,  $[D]$ , is the constitutive relation matrix for the interface.

### Equivalent Nodal Force Vector

Equivalent nodal force vector,  $\{Q\}_e$ , for the element is given as:

$$\{Q\}_e = \int [N]^T \begin{bmatrix} f_u \\ f_v \\ f_w \end{bmatrix} dA \quad (12)$$

where, elements of  $[N]$  contain shape functions and  $\sin n\theta$  or  $\cos n\theta$ .

### CONSTITUTIVE MODEL

In this study, the pile was assumed to be linearly elastic. Nonlinearity of the soil medium was represented by bilinear model, in which yield surface is described by von-Mises yield criterion, in term of yield function,  $F$ , as:

$$F = J_{D2} - \sigma_y = 0 \quad (13)$$

where,  $\sigma_y$  indicates an experimentally determined yield stress, and  $J_{D2}$  is the second deviatoric stress invariant. In terms of the stresses, von-Mises criterion is:

$$F = [(1/2)(\sigma_r - \sigma_\theta)^2 + (1/2)(\sigma_\theta - \sigma_z)^2 + (1/2)(\sigma_z - \sigma_r)^2 + 3(\tau_{r\theta})^2 + 3(\tau_{r\theta})^2 + 3(\tau_{rz})^2]^{1/2} - \sigma_y = 0 \quad (14)$$

It is also expressed as:

$$F = \sigma' - \sigma_y = 0 \quad (15)$$

where,  $\sigma'$  is known as the effective or equivalent stress, and in fact corresponds to uniaxial yield value. Effective or equivalent strain,  $\epsilon'$ , corresponding to the effective or equivalent stress,  $\sigma'$ , is given in terms of co-ordinate strains as:

$$\epsilon' = \sigma'/E = \{1/[\sqrt{2}(1+\nu)]\} \{(\epsilon_r - \epsilon_\theta)^2 + (\epsilon_r - \epsilon_z)^2 + (\epsilon_z - \epsilon_\theta)^2 + (3/2)[(\gamma_{r\theta})^2 + (\gamma_{rz})^2 + (\gamma_{\theta z})^2]\}^{1/2} \quad (16)$$

From Eq. 15 and Eq. 16, von-Mises yield criterion can be written in terms of effective strain,  $\epsilon'$ , and yield strain,  $\epsilon_y$ , as:

$$F = E(\epsilon' - \epsilon_y) = 0 \quad (17)$$

Unloading was assumed to take place in a purely elastic manner, with elastic components of strain being independent of plastic deformation.

Nonlinearity of interface was also modelled using bilinear relationship. The shear stress components in  $\{\sigma\}_e$  vector, and shear strain components in  $\{\epsilon\}_e$  vector were added vectorially to get the resultant shear stress,  $\sigma'_s$ , and resultant shear strain,  $\epsilon'_s$ . The interface was considered to yield when the resultant shear stress exceeds the yield value of shear stress for the interface.

### Material Properties

The pile was assumed to be linearly elastic, defined by Young's modulus  $E$ , and Poisson's ratio  $\nu$ . The soil

behavior was treated as bilinear with moduli,  $E_1$  and  $E_2$ , before and after yielding, respectively, with Poisson's ratio  $\nu$ . Interface behavior was also modeled as bilinear, with shear stiffnesses,  $k_{s1}$  and  $k_{s2}$ , before and after yielding, respectively. The normal stiffness,  $k_n$ , of the interface was assumed to be constant.

### EFFECT OF CYCLIC LOADING (POULOS, 1982)

For a clay loaded under undrained conditions, cyclic loading may have two important effects. It may lead to reduction in soil modulus and undrained shear strength, which, in turn leads to reduction in yield stress,  $\sigma_y$ , yield shear stress,  $\tau_y$  of interface and interface shear stiffness,  $k_s$ . These effects which are associated with the generation of excess pore pressure during the cyclic loading process, should be taken into account while analysing the response of a pile to cyclic loading. The most satisfactory means of performing this analysis would be to consider each cycle of loading separately, with soil parameters being progressively adjusted after each cycle.

A convenient means of defining the effects of cyclic loading on soil parameters is in terms of degradation factors, which express the ratio of the parameter for cyclic loading to the value of parameter for a single static load application. The degradation factor,  $D_e$ , for soil modulus and  $D_p$ , for yield pressure are therefore defined as:

$$D_e = E_1/E_2 = k_{s1}/k_{s2} \quad \text{and} \quad D_p = \sigma_{y1}/\sigma_{y2} = \tau_{y1}/\tau_{y2} \quad (18)$$

in which,  $E_1$  and  $E_2$  are the soil moduli,  $k_{s1}$  and  $k_{s2}$  are interface shear stiffnesses,  $\sigma_{y1}$  and  $\sigma_{y2}$  are the yield pressures, and,  $\tau_{y1}$  and  $\tau_{y2}$  are yield shear stresses at interface, for static and cyclic loading respectively.

From the relatively small amount of data available, the degradation factors for a saturated clay under undrained conditions appear to be related to the cyclic strain. Based on the data summarized by Idriss, et al. (1978), for a San Francisco Bay mud, the degradation factors  $D_p$  and  $D_e$  are expressed as follows:

$$\alpha = D_e = D_p = N^t \quad (19)$$

in which,  $\alpha$  represents degradation factor,  $N$  represents number of cycles, and  $t$  represents degradation parameter depending on cyclic normal strain.

Figure 1 shows a plot of degradation parameter,  $t$ , versus cyclic strain ratio,  $\epsilon_c/\epsilon_{cr}$ , derived from the data, presented by Idriss, et al. (1978).  $\epsilon_c$  is the cyclic strain and  $\epsilon_{cr}$  is a reference value of cyclic strain. The cyclic degradation behavior of different soil types can be obtained by altering the value of cyclic reference strain,  $\epsilon_{cr}$ . The smaller the value of  $\epsilon_{cr}$ , the smaller is the cyclic strain necessary to produce a given amount of degradation, i.e., more susceptible is the soil to cyclic degradation.

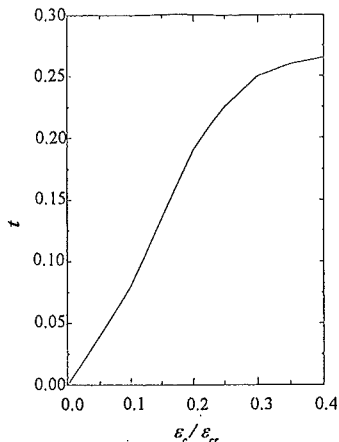


Fig. 1 Degradation Parameter  $t$  (Poulos, 1982)

### ITERATIVE PROCEDURE

The effect of cyclic loading was incorporated by allowing the reduction of soil modulus and yield stress, with increasing cyclic strain, at every cycle. The hysteretic behavior in a typical stress-strain curve under the action of loading, unloading and subsequent reloading is shown in Fig. 2 and Fig. 3. This type of modelling of the nonlinear behavior of soil not only helps in tracing the loading and unloading paths, but also estimates the cyclic response of pile in a more realistic manner. The development of the procedure was based on the evaluation of stresses and strains pertaining to a constant stiffness, for various iterative steps at every cycle. The difference between the computed stress and the stress that is consistent with the computed strain was used to compute the load vector for next iteration. Because, constant stiffness was employed in all the iterations, this procedure offers a unique advantage for analysing a non-linear problem. Various iterative steps involved in the analysis for loading and unloading of each cycle are given below.

#### Loading

For given loading, elastic analysis based on initial tangent modulus of bilinear relationship was performed to obtain amplitudes of nodal displacements in various harmonics. Iterative steps involved in the analysis are given below :

1. Stresses and strains in the soil element and interface element were obtained from:

$$\{\epsilon\}_e = [B]\{\delta\}_e \quad \text{and} \quad \{\sigma\}_e = [D]\{\epsilon\}_e \quad (20)$$

The equivalent strain,  $\epsilon^e$ , at any point  $(r, \theta, z)$ , in the soil continuum is given as:

$$\epsilon^e = \{1/[\sqrt{2}(1 + \nu)]\} \{(\epsilon_r - \epsilon_\theta)^2 + (\epsilon_r - \epsilon_z)^2 + (\epsilon_\theta - \epsilon_z)^2 + (3/2)[(\gamma_{r\theta})^2 + (\gamma_{r\theta})^2 + (\gamma_{rz})^2]\}^{1/2} \quad (21)$$

For interface elements, the shear strain components in  $\{\epsilon\}_e$  vector, were added vectorially to get resultant shear strain  $\epsilon^e$ . From Fig. 1, degradation parameter,  $t$ , was determined for the strain ratio  $\epsilon^e/\epsilon_{cr}$ . The degradation factor,  $\alpha$ , was computed using the following relation:

$$\alpha = N^t \quad (22)$$

2. Extra stress vector,  $\{\Delta\sigma\}$ , which is the difference between the computed stress and the stress consistent with the computed strain,  $\epsilon^e$ , was evaluated by using the expressions given in the Appendix.
3. These values of  $\{\Delta\sigma\}_e$  were expanded in the form of full range finite harmonic series. The expanded form of  $\{\Delta\sigma\}_e$  is expressed as:

$$\{\Delta\sigma(\theta)\}_e = \sum_{n=0}^L \{\Delta\sigma_n\}_e \quad (23)$$

where  $\{\Delta\sigma(\theta)\}_e$  is the extra stress vector at any angle  $\theta$ , in finite harmonic series form and  $\{\Delta\sigma_n\}_e$  is the extra stress vector in the  $n$ th harmonic after expansion.

4. The corresponding nodal force vector,  $\{\Delta Q_n\}_e$ , in  $n$ th harmonic for the next iteration is given as follows,

$$\{\Delta Q_n\}_e = \int_v [B_n]^T \{\Delta\sigma_n\}_e dv \quad (24)$$

and for interface element,

$$\{\Delta Q_n\}_e = \int_s [B_n]^T \{\Delta\sigma_n\}_e ds \quad (25)$$

5. Finite element analysis for the assembled correcting force vector was performed harmonicwise, with no change in the stiffness matrix.
6. This analysis gives increments in the amplitudes of nodal displacements,  $\{\Delta\delta_n\}$ . The revised amplitudes of nodal displacements at a point were obtained from the following expression:

$$\{\delta_n\} = \{\delta_n\} + \{\Delta\delta_n\} \quad (26)$$

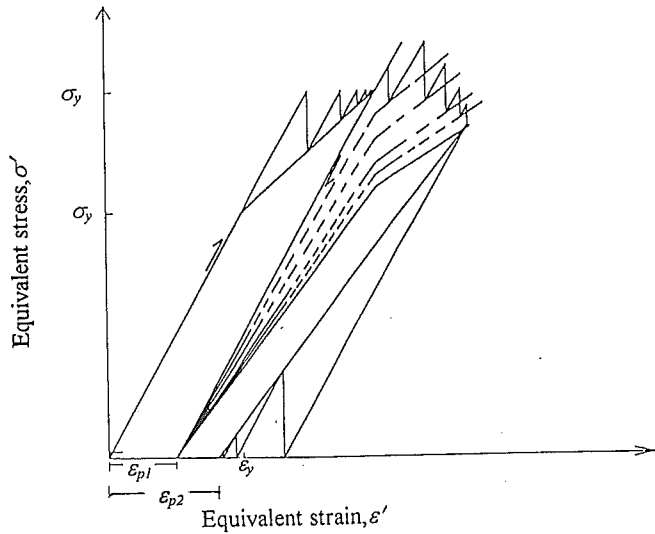


Fig. 2 Representation of Analysis for One-Way Cyclic Loading

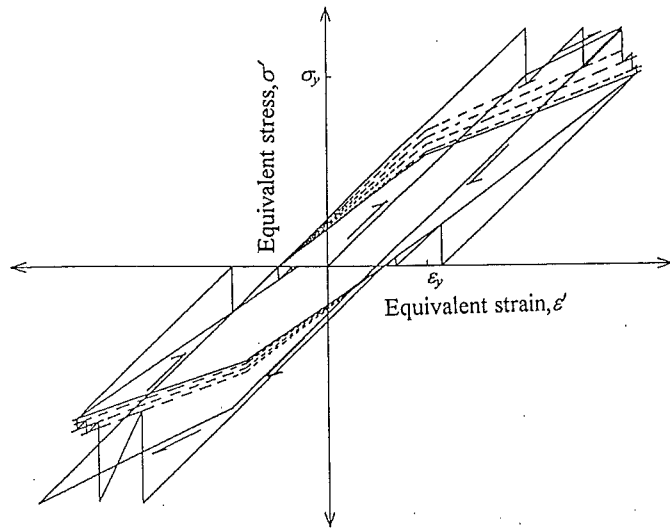


Fig. 3 Representation of Analysis for Two-Way Cyclic Loading

7. The procedure was repeated until satisfactory convergence was obtained.

**Unloading**

The same iterative procedure was used for unloading. Final set of values of degradation factors,  $\alpha'$ , were used in unloading, and as the stresses in the soil were reduced in the process, its behavior was linear.

**VALIDATION**

The validation of analysis was carried out by comparing with the results of model tests conducted by Georgiadis, et al. (1992), on an aluminium pile of length 500 mm embedded in soft to medium clay, (undrained shear strength  $C_u = 28 \text{ kN/m}^2$ ) subjected to cyclic lateral load. The flexural stiffness  $EI$  of pile was  $0.2 \text{ kNm}^2$ .

The following soil parameters were found to give best fit to static results:  $E_1 = 2800 \text{ kN/m}^2$ ;  $E_2/E_1 = 0.2$ ;  $\nu = 0.45$ ;  $\epsilon_y = 0.002$ . A value of  $\epsilon_{cr} = 0.02$  as suggested by Poulos (1982) for soft clay was used in the analysis.

Figure 4 compares experimental and predicted load-deflection behavior for  $N=1$  and  $N=10$  cycles. Distribution of bending moment along depth for load of 146 N is shown in Fig. 5. Maximum percentage error is of the order 13.0 to 17.0, and this shows a fairly good agreement.

**RESULTS OF PARAMETRIC STUDY**

Analyses were carried out for two pile-soil systems (Case 1,  $L/d = 10$ , and Case 2,  $L/d = 25$ ), subjected to 100 cycles of one way and two way cyclic loading. In both cases, soil was assumed homogeneous. Pile flexibility factor,  $k = EI/E_s L^4 = 10^{-4}$ , was maintained in both cases. Material properties are shown in Table 1. Observed ultimate loads  $H_w$ , were expressed as a fraction of ultimate soil resistance,  $H_{ur}$  where  $H_w = \sigma_y dL$ .

**Case-1**

Figure 6 shows the variation of load with displacement for static and cyclic loading. There is a substantial increase in the top displacement after specified cycles of loading. Yielding takes place at 120 kN ( $H_w/H_{ur} = 0.611$ ) for one-way cyclic loading, and at 90 kN ( $H_w/H_{ur} = 0.458$ ) for two-way cyclic loading. Variation of load with moment is shown in Fig. 7. Maximum increase in the maximum moment after 100 cycles is 11.6% for one-way cyclic loading, and 22.0% for two-way cyclic loading. Figure 8 shows the comparison between distribution of moment along the length of pile, at cycle 1 and cycle 100, for 90 kN lateral load. Effect of cyclic loading was observed to be more pronounced in the lower half of the pile.

Table 1 Material Properties of Pile, Soil and Interface Media

Pile	Soil	Interface
$E_p = 2.0E8 \text{ kN/m}^2$	case - 1 $E_1 = 982 \text{ kN/m}^2$ and $E_2 = 0$ case- 2 $E_1 = 4267 \text{ kN/m}^2$ and $E_2 = 0$	$k_{s1} = 1000 \text{ kN/m}^3$ $k_{s2} = 1000 \text{ kN/m}^3$ $k_{s2} = 0$
$\nu = 0.15$	$\nu_s = 0.45$	
Diameter = 1 m	$\epsilon_y = 0.02$	$\epsilon_y = 0.02$
Length case - 1 = 10 m and case - 2 = 25 m.	$\epsilon_{cr} = 0.02$	$\epsilon_{cr} = 0.02$

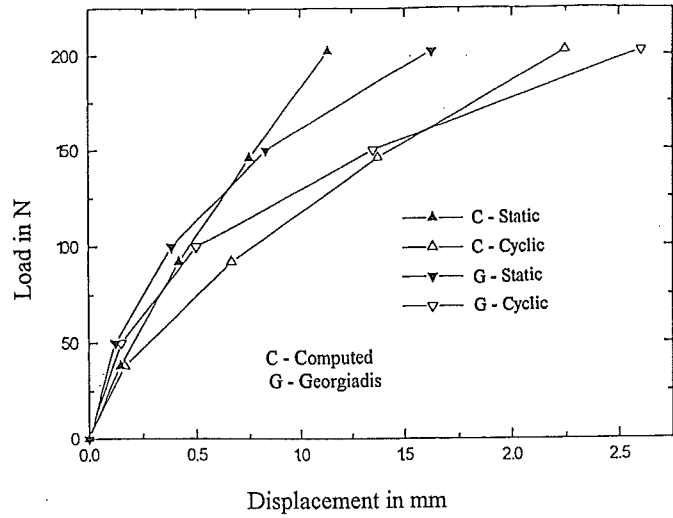


Fig. 4 Comparison of Load-Deflection Behavior

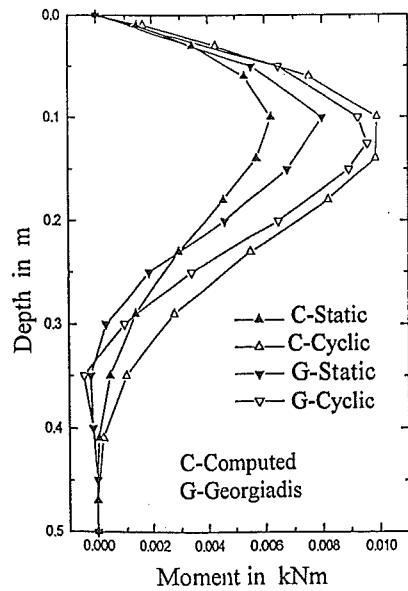


Fig. 5 Comparison of Distribution of Bending Moment

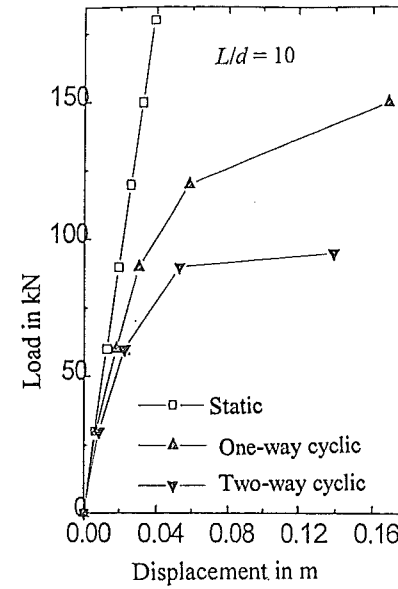


Fig. 6 Load Displacement Relationship

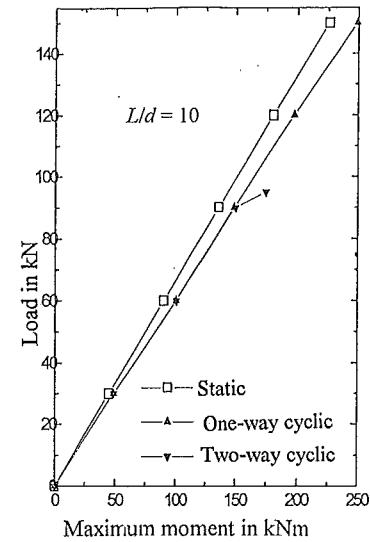


Fig. 7 Load Moment Relationship

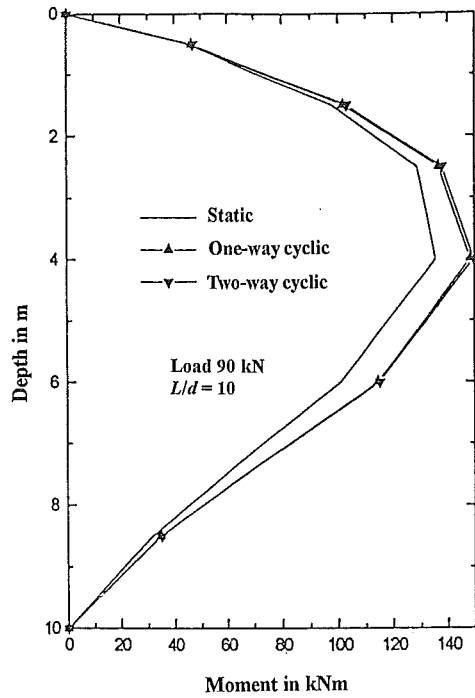


Fig. 8 Moment Distribution along Pile Length

Table 2 Ultimate Load,  $H_u$  as a Fraction of Ultimate Soil resistance  $H_{ur}$

Pile	$H_u/H_{ur}$ for one-way cyclic loading	$H_u/H_{ur}$ for two-way cyclic loading
Case 1 - $L/d = 10$	0.611	0.458
Case 2 - $L/d = 25$	0.526	0.422

Case-2

Figure 9 shows the plot of load versus displacement for static and cyclic loading. Maximum increase in the top displacement after 100 cycles is 130% at 1200 kN ( $H_u/H_{ur} = 0.562$ ) for one-way cyclic loading, and 301% at 900 kN ( $H_u/H_{ur} = 0.422$ ) for two-way cyclic loading. Yielding takes place at 1200 kN for one-way cyclic loading, and at 900 kN for two-way cyclic loading. Plot of load versus moment is shown in Fig. 10. Increase in maximum moment after 100 cycles is 30%. Figure 11 shows the comparison between distribution of moment along the length of pile, at cycle 1 and cycle 100, for 500 kN lateral load. The effect of cyclic loading was observed to be more pronounced in the lower half of the pile. The ratios of  $H_u/H_{ur}$  for both pile-soil systems are reported in Table 2.

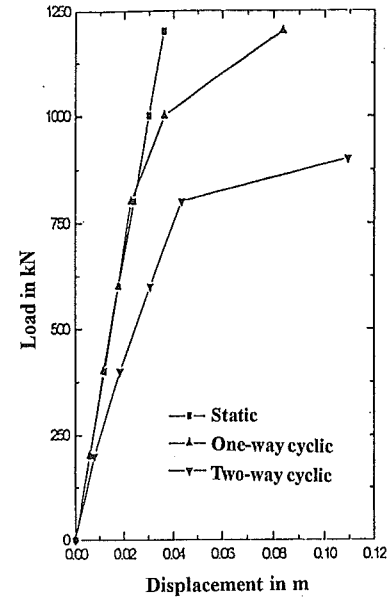


Fig. 9 Load Displacement Relationship

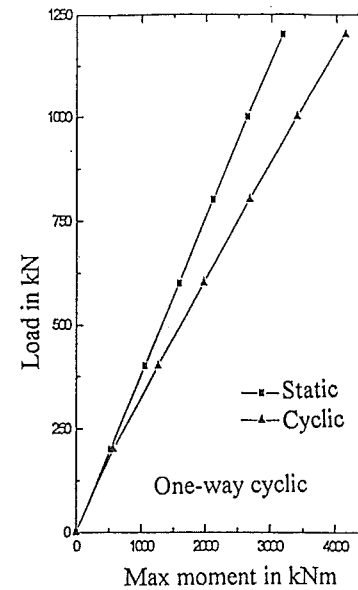


Fig. 10 Load Moment Relationship

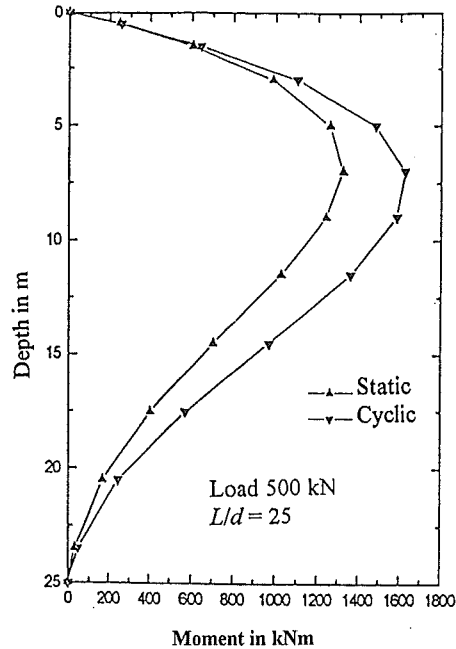


Fig. 11 Moment Distribution along Pile Length

### CONCLUSIONS

The analysis presented considers two important factors, namely, degradation of soil modulus and yield stress, and accumulation of permanent displacements. It reproduces the observed characteristics of pile behavior under cyclic loading reasonably well, namely, an increase in deflection and moment with increasing number of cycles and increasing load level, and a decrease in ultimate lateral load capacity. Apart from the usual data required for a static analysis, the only additional data required for a cyclic analysis are the variation of degradation parameter,  $t$ , with cyclic strain. The range values of  $\varepsilon_y$ , as suggested by Poulos are 0.01 to 0.02 for soft clay and 0.001 to 0.002 for stiff clay. The following conclusions are drawn from the above study:

1. Effect of two-way cyclic loading is higher compared to one-way cyclic loading, when displacements are considered, while, one-way cyclic loading and two-way cyclic loading have the same effect on bending moments in the pile.
2. There is significant increase in the top displacement of piles, whereas, maximum increase in maximum moment was only 30% for both one-way cyclic loading and two-way cyclic loading.
3. The ultimate lateral load capacity for cyclic loading was observed to be 56% to 61% of  $H_{ur}$  for one-way cyclic loading, and 42% to 46% of  $H_{ur}$  for two-way cyclic loading.
4. The moment distribution along the depth of pile showed that more increase in moment occurs in the lower half of the pile under cyclic loading condition.

### APPENDIX: COMPUTATION OF EXTRA STRESS VECTOR

#### Loading

The extra stress vector,  $\{\Delta\sigma\}_e$ , for first iteration is computed as follows:  
When  $\varepsilon'$  is less than yield strain  $\varepsilon_y$ ,

$$\{\Delta\sigma\}_e = (1-\alpha)[D]\{\varepsilon\}_e$$

and for interface element

$$\{\Delta\sigma\}_e = (1-\alpha)[D_m][D]\{\varepsilon\}_e \quad (A-1)$$

where,

$$[D_m] = \begin{bmatrix} 1 & 0 & 0 \\ 0 & 1 & 0 \\ 0 & 0 & 0 \end{bmatrix} \quad (A-2)$$

When  $\varepsilon'$  is greater than yield strain  $\varepsilon_y$ ,

$$\{\Delta\sigma\}_e = \frac{E_1 - E_s}{E_1}[D]\{\varepsilon\}_e$$

and for interface element

$$\{\Delta\sigma\}_e = \frac{k_{s1} - k_{ss}}{k_{s1}}[D_m][D]\{\varepsilon\}_e \quad (A-3)$$

where,  $E_1$  and  $E_s$ , are soil moduli before and after yielding,  $k_{s1}$  and  $k_{s2}$ , are interface shear stiffnesses before and after yielding,  $E_s$  and  $k_{ss}$  are the secant moduli, corresponding to strain  $\varepsilon'$ , given by:

$$E_s = \frac{\alpha E_1 \varepsilon_y + \alpha E_2 (\varepsilon' - \varepsilon_y)}{\varepsilon'}$$

$$k_{ss} = \frac{\alpha k_{s1} \varepsilon_y + \alpha k_{s2} (\varepsilon' - \varepsilon_y)}{\varepsilon'} \quad (A-4)$$

The extra stress vector,  $\{\Delta\sigma\}_e$  for next iterations is given by the following expressions:

If  $\varepsilon'$  is less than yield strain  $\varepsilon_y$ , then

$$\{\Delta\sigma\}_e = (1-\alpha)[D]\{\Delta\varepsilon\}_e + (\alpha - \alpha')[D]\{\varepsilon\}_e$$

and for interface element

$$\{\Delta\sigma\}_e = (1-\alpha)[D_m][D]\{\Delta\varepsilon\}_e + (\alpha - \alpha')[D_m][D]\{\varepsilon\}_e \quad (A-5)$$

If  $\varepsilon'$  is greater than yield strain,  $\varepsilon_y$ , and point is not yielded in previous iteration, then:

$$\{\Delta\sigma\}_e = \frac{E_1 - \Delta\bar{\sigma}}{E_1}[D]\{\Delta\varepsilon\}_e + (\alpha - \alpha') \frac{E_s}{E_1}[D]\{\varepsilon\}_e \quad (A-6)$$

where,

$$\Delta\bar{\sigma} = \alpha E_1 (\varepsilon_y + \Delta\varepsilon' - \varepsilon) + \alpha E_2 (\varepsilon' - \varepsilon_y) \quad (A-7)$$

and for interface element:

$$\{\Delta\sigma\}_e = \frac{k_{s1} - \frac{\Delta\bar{\tau}}{\Delta\varepsilon^1}}{k_{s1}} [D_m][D]\{\Delta\varepsilon\}_e + (\alpha - \alpha') \frac{k_{ss}}{k_{s1}} [D_m][D]\{\varepsilon\}_e \quad (\text{A-8})$$

where,

$$\Delta\bar{\tau} = \alpha k_{s1}(\varepsilon_y + \Delta\varepsilon^1 - \varepsilon) + \alpha k_{s2}(\varepsilon^1 - \varepsilon_y) \quad (\text{A-9})$$

If  $\varepsilon^1$  is greater than yield strain,  $\varepsilon_y$ , and point is yielded in previous iteration, then :

$$\{\Delta\sigma\}_e = \frac{E_1 - \alpha E_2}{E_1} [D]\{\Delta\varepsilon\}_e + (\alpha - \alpha') \frac{E_s}{E_1} [D]\{\varepsilon\}_e \quad (\text{A-10})$$

and for interface element

$$\{\Delta\sigma\}_e = \frac{k_{s1} - \alpha k_{s2}}{k_{s1}} [D_m][D]\{\Delta\varepsilon\}_e + (\alpha - \alpha') \frac{k_{ss}}{k_{s1}} [D_m][D]\{\varepsilon\}_e \quad (\text{A-11})$$

### Unloading

For unloading, the extra stress vector,  $\{\Delta\sigma\}_e$ , is calculated as:

$$\{\Delta\sigma\}_e = (1 - \alpha)[D]\{\Delta\varepsilon\}_e$$

and for interface element:

$$\{\Delta\sigma\}_e = (1 - \alpha)[D_m][D]\{\Delta\varepsilon\}_e \quad (\text{A-12})$$

### Loading in Opposite Direction

The extra stress vector,  $\{\Delta\sigma\}_e$ , for first iteration is computed as follows :

Calculate the degradation parameter,  $\alpha'$ , for the equivalent strain,  $\varepsilon^1$ . If  $\alpha'$  is less than  $\alpha$ , then set  $\alpha = \alpha'$ .

When  $\varepsilon^1$  is less than yield strain,  $\varepsilon_y$ ,

$$\{\Delta\sigma\}_e = (1 - \alpha)[D]\{\varepsilon\}_e$$

and, for interface element,

$$\{\Delta\sigma\}_e = (1 - \alpha)[D_m][D]\{\varepsilon\}_e \quad (\text{A-13})$$

When  $\varepsilon^1$  is greater than yield strain,  $\varepsilon_y$ ,

$$\{\Delta\sigma\}_e = \frac{E_1 - E_s}{E_1} [D]\{\varepsilon\}_e$$

and, for interface element,

$$\{\Delta\sigma\}_e = \frac{k_{s1} - k_{ss}}{k_{s1}} [D_m][D]\{\varepsilon\}_e \quad (\text{A-14})$$

where,  $E_s$  and  $k_{ss}$  are the secant moduli, corresponding to strain,  $\varepsilon^1$  and are given as:

$$E_s = \frac{\alpha E_1 \varepsilon_y + \alpha E_2 (\varepsilon^1 - \varepsilon_y)}{\varepsilon^1} \quad (\text{A-15})$$

$$k_{ss} = \frac{\alpha k_{s1} \varepsilon_y + \alpha k_{s2} (\varepsilon^1 - \varepsilon_y)}{\varepsilon^1}$$

The extra stress vector,  $\{\Delta\sigma\}_e$ , for next iterations is given by the following expressions.

Set the degradation parameter in last iteration as  $\alpha$ . Calculate new degradation parameter,  $\alpha'$ , for equivalent strain,  $\varepsilon^1$ .

1. If  $\alpha'$  greater than  $\alpha$ , only  $\alpha$  will be considered.

a) If the point has failed in earlier iteration,

$$\{\Delta\sigma\}_e = \frac{E_1 - \alpha E_2}{E_1} [D]\{\Delta\varepsilon\}_e$$

and, for interface element,

$$\{\Delta\sigma\}_e = \frac{k_{s1} - \alpha k_{s2}}{k_{s1}} [D_m][D]\{\Delta\varepsilon\}_e \quad (\text{A-16})$$

b) If the point has not failed in earlier iteration, then

I) for  $\varepsilon^1$  less than yield strain,  $\varepsilon_y$ ,

$$\{\Delta\sigma\}_e = (1 - \alpha)[D]\{\Delta\varepsilon\}_e$$

and, for interface element,

$$\{\Delta\sigma\}_e = (1 - \alpha)[D_m][D]\{\Delta\varepsilon\}_e \quad (\text{A-17})$$

II) for,  $\varepsilon^1$ , greater than yield strain,  $\varepsilon_y$ ,

$$\{\Delta\sigma\}_e = \frac{E_1 - E_s}{E_1} [D]\{\varepsilon\}_e$$

and, for interface element,

$$\{\Delta\sigma\}_e = \frac{k_{s1} - k_{ss}}{k_{s1}} [D_m][D]\{\varepsilon\}_e \quad (\text{A-18})$$

where,  $E_s$  and  $k_{ss}$  are the secant moduli, corresponding to strain,  $\varepsilon^1$  and are given as:

$$E_s = \frac{\alpha E_1 \varepsilon_y + \alpha E_2 (\varepsilon^1 - \varepsilon_y)}{\varepsilon^1}$$

$$k_{ss} = \frac{\alpha k_{s1} \varepsilon_y + \alpha k_{s2} (\varepsilon^1 - \varepsilon_y)}{\varepsilon^1} \quad (\text{A-19})$$

2. If  $\alpha'$  is less than  $\alpha$ , both should be considered.

a) If the point has failed in earlier iteration,

$$\{\Delta\sigma\}_e = \frac{E_1 - \alpha E_2}{E_1} [D]\{\Delta\varepsilon\}_e + (\alpha - \alpha') \frac{E_s}{E_1} [D]\{\varepsilon\}_e \quad (\text{A-20})$$

and, for interface element,

$$\{\Delta\sigma\}_e = \frac{k_{s1} - \alpha k_{s2}}{k_{s1}} [D_m][D]\{\Delta\varepsilon\}_e + (\alpha - \alpha') \frac{k_{ss}}{k_{s1}} [D_m][D]\{\varepsilon\}_e \quad (\text{A-21})$$

where,

$$E_s = \frac{E_1 \varepsilon_y + E_2 (\varepsilon^1 - \varepsilon_y)}{\varepsilon^1}$$



$$\text{and, } k_{ss} = \frac{\alpha k_{s1} \varepsilon_y + \alpha k_{s2} (\varepsilon' - \varepsilon_y)}{\varepsilon'}$$

b) If the point has not failed in earlier iteration,

I) for  $\varepsilon'$ , less than yield strain,  $\varepsilon_y$ ,

$$\{\Delta\sigma\}_e = (1 - \alpha)[D]\{\Delta\varepsilon\}_e + (\alpha - \alpha')[D]\{\varepsilon\}_e$$

and, for interface element,

$$\{\Delta\sigma\}_e = (1 - \alpha)[D_m][D]\{\Delta\varepsilon\}_e + (\alpha - \alpha')[D_m][D]\{\varepsilon\}_e \quad (\text{A-22})$$

II) for  $\varepsilon'$  greater than yield strain,  $\varepsilon_y$ ,

$$\{\Delta\sigma\}_e = \frac{E_1 - \Delta\bar{\sigma}}{\Delta\varepsilon'} [D]\{\Delta\varepsilon\}_e + (\alpha - \alpha') \frac{E_2}{E_1} [D]\{\varepsilon\}_e \quad (\text{A-23})$$

$$\text{where, } \Delta\bar{\sigma} = \alpha E_1 (\varepsilon_y + \Delta\varepsilon' - \varepsilon) + \alpha E_2 (\varepsilon' - \varepsilon_y) \quad (\text{A-24})$$

$$\text{and, } E_s = \frac{E_1 \varepsilon_y + E_2 (\varepsilon' - \varepsilon_y)}{\varepsilon'}$$

for interface element,

$$\{\Delta\sigma\}_e = \frac{k_{s1} - \Delta\bar{\sigma}}{\Delta\varepsilon'} [D_m][D]\{\Delta\varepsilon\}_e + (\alpha - \alpha') \frac{k_{ss}}{k_{s1}} [D_m][D]\{\varepsilon\}_e \quad (\text{A-25})$$

$$\text{where, } \Delta\bar{\sigma} = \alpha k_{s1} (\varepsilon_y + \Delta\varepsilon' - \varepsilon) + \alpha k_{s2} (\varepsilon' - \varepsilon_y) \quad (\text{A-26})$$

$$\text{and, } k_{ss} = \frac{\alpha k_{s1} \varepsilon_y + \alpha k_{s2} (\varepsilon' - \varepsilon_y)}{\varepsilon'}$$

## REFERENCES

- BURAGOHAJ, D. N. and SHAH, V. L. (1977). Curved interface elements for interaction problems. *Proceedings of the International Symposium on Soil-Structure Interaction*, India, pp. 197-202.
- GEORGIADIS, M.; ANAGNOSTOPOULOS, C.; and SAFLEKOU, S. (1992). Cyclic lateral loading of piles in soft clay. *Geotechnical Engineering*, Vol. 23, pp. 47-60.
- IDRISS, I.M.; DOBRY, R.; and SINGH, R.D. (1978). Nonlinear behaviour of soft clays during cyclic loading. *Journal of Geotechnical Engineering Division*, ASCE, Vol. 104, GT12, pp. 1427-1447.
- KUHLEMEYER, R. L. (1979). Static and dynamic laterally loaded floating piles. *Journal of Geotechnical Engineering Division*, ASCE, Vol. 105, No. GT2, pp. 289-304.
- LONG, J.H. and VENNESTE, G. (1994). Effects of cyclic lateral loads on piles in sand. *Journal of Geotechnical Engineering Division*, ASCE, Vol. 120, No. GT2, pp. 289-304.
- POULOS, H. G. (1982). Single pile response to cyclic lateral loads. *Journal of Geotechnical Engineering*, Vol. 108, GT3, pp. 711-731.
- RANDOLPH, M. F. (1981). Response of flexible pile to lateral loads. *Geotechnique*. Vol. 31, No. 2, pp. 247-259.

## USING GEOTECHNICAL DATABASE FOR MODELING SPATIAL VARIABILITY OF SOIL PROPERTIES

X-X. Li<sup>1</sup> and S. Hayashi<sup>2</sup>

### ABSTRACT

This paper presents a probabilistic model to determine bore-hole spacing and spatial variability of soil properties during site investigation. Using this model, it is possible to evaluate the bore-hole spacing and important soil properties for the estimation error used in reliability-design. However, this model requires correlation distance and variance of soil properties as important data input. The geotechnical data-base system for Saga plain, Japan is used to establish the relationship between these statistical variables and soil characteristics, such as, undrained shear strength, layer thickness, etc. The exploration spacing for different estimation errors is suggested for site investigation.

### INTRODUCTION

Site exploration gives important information about the ground profile and important soil properties. The accuracy of such information, however, depends upon the number of sample, the quality of test data and the location of sample. If the information from such exploration is limited and there is a need to estimate the ground information or the soil properties at unsampled location, one may ask how reliable is the estimate to meet the safety requirement in the design. Of course, carrying out additional exploration or increasing the number of samples can reduce uncertainty due to spatial variability of soil properties. However, sometimes it will result in what is called "wasteful redundancy" in the information collected. So, it is important to choose an optimum exploration spacing that gives the best estimate of the ground profile and the soil properties considering overall aspects of safety and economy.

Although the ground thickness or engineering soil properties at an unsampled location on the ground can be directly estimated from neighboring bore-holes either by interpolation or geotechnical judgement, one cannot determine however the estimation errors in such determinative procedures. The predictive geostatistical procedures, such as ordinary and universal kriging based on the theory of regionalized variables (Matheron, 1971) are best suited for this purpose; not only that they give better interpolation than determinative methods but also evaluate estimation errors for such interpolations. Kriging is a collection of generalized liner regression techniques for minimizing an estimation error obtained from a priori model for a covariance (Journel and Huijbregts, 1978; and Deutsch and Journel, 1998). Although kriging was initially introduced to provide estimates for unsampled values (Krige, 1951; and Matheron, 1971), it is being used increasingly to build probabilistic models of uncertainty about these unknown values (Journel, 1989).

Based on the kriging principle mentioned above, this paper presents a simple probabilistic model to evaluate unknown value and estimation error of soil properties at unsampled location in the ground. This model can also be used to evaluate the borehole spacing. The statistical parameters, namely, a correlation distance and variance for this model are established using a geotechnical database system for Saga plain, Japan. Finally, the exploration spacing for different values of estimation error is suggested for the site investigation.

### PROBABILISTIC ESTIMATION MODEL

Predictive geostatistics characterize any unsampled value of soil property  $w$  as a random variable  $W$ . The random variable  $W$ , and more specifically its probability distribution (mean and standard deviation), is usually location-dependent (Webster and Burgess, 1980); hence this variable is denoted as  $W(u)$  where  $u$  is a location coordinates vector.

<sup>1</sup> Lecturer, Institute of Lowland Technology, Saga University, 1 Honjo, Saga, 840-8502, Japan.

<sup>2</sup> Professor, Institute of Lowland Technology, Saga University, 1 Honjo, Saga, 840-8502, Japan.

Note: Discussion is open until 1 July 1999. This paper is part of the *Geotechnical Engineering Journal*, Vol. 30, No. 1, April 1999. Published by the Southeast Asian Geotechnical Society, ISSN 0046-5828.